


Strength and typicality of nonlocality in multisetting and multipartite Bell scenarios

Anna de Rosier,¹ Jacek Gruca,^{1,2} Fernando Parisio,³ Tamás Vértesi,⁴ and Wiesław Laskowski ^{1,2}

¹*Institute of Theoretical Physics and Astrophysics, Faculty of Mathematics, Physics and Informatics, University of Gdańsk, 80-308 Gdańsk, Poland*

²*International Centre for Theory of Quantum Technologies, University of Gdańsk, 80-308 Gdańsk, Poland*

³*Departamento de Física, Federal University of Pernambuco, Recife, PE 50670-901, Brazil*

⁴*MTA Atomki Lendület Quantum Correlations Research Group, Institute for Nuclear Research, Hungarian Academy of Sciences, P.O. Box 51, H-4001 Debrecen, Hungary*



(Received 7 June 2019; published 16 January 2020)

In this work we investigate the probability of violation of local realism under random measurements in parallel with the strength of these violations as described by resistance to white noise admixture. We address multisetting Bell scenarios involving up to seven qubits. As a result, in the first part of this manuscript, we report statistical distributions of a quantity reciprocal to the critical visibility for various multipartite quantum states subjected to random measurements. The statistical relevance of different classes of multipartite tight Bell inequalities violated with random measurements is investigated. We also introduce the concept of typicality of quantum correlations for pure states as the probability to generate a nonlocal behavior with both random state and measurement. Although this typicality is slightly above 5.3% for two qubits, for a modest increase in the number of involved particles it quickly surpasses 99.99%.

DOI: [10.1103/PhysRevA.101.012116](https://doi.org/10.1103/PhysRevA.101.012116)

I. INTRODUCTION

Quantum entanglement is at the core of the new technologies driven by quantum physics. Its direct manifestation in our classical world are correlations between measurement results which are much stronger than what is possible within classical physics. The probability of violation of local realism under random measurements, proposed in [1], has gained considerable attention as an operational measure of nonclassicality of quantum states [2]. It has been demonstrated both numerically [3–5] and analytically [2,6] that this quantity is a good candidate for a nonlocality measure. What is more, in [6] it was proved that this quantifier satisfies some natural properties and expectations for an operational measure of nonclassicality, e.g., invariance under local unitaries.

In our approach to quantify nonlocality there are no prior assumptions about specific Bell inequalities. Instead we consider a joint probability distribution that is equivalent to the analysis of a full set of tight inequalities in a given Bell scenario (see also the recent machine learning approach in Ref. [7] to this problem). The probability of violation for a state ρ is therefore defined as

$$\mathcal{P}_V(\rho) = \int f(\rho, \Omega) d\Omega, \quad (1)$$

where the integration variables Ω correspond to all setting parameters that can vary within a Bell scenario and with

$$f(\rho, \Omega) = \begin{cases} 1, & \text{if settings lead to violations} \\ & \text{of local realism,} \\ 0, & \text{otherwise.} \end{cases} \quad (2)$$

Quantum correlations allow one to explore the foundations of quantum mechanics and at the same time are also at the basis of various so-called device-independent applications such as device-independent quantum key distribution, randomness certification, dimension witnesses, or self-testing (see, e.g., Ref. [8] for details). They require states that strongly violate Bell inequalities; however, the concept of “strength of violation” is controversial in the literature. Although definition (1) fairly captures the nonclassical extent of a state, it seems useful to put it together with another quantitative description which addresses the “fragility” of this nonclassicality against noise. Our approach enables us to report the probability that a state exhibits nonclassical correlations when random measurements are performed on it, and simultaneously measure the resistance to noise or to decoherence embodied by these quantum correlations [9,10].

However, in order to fully harness these nonlocal quantum correlations, it is very important to understand the geometry of the set of quantum correlations, and in particular how it relates to the set which can be merely described in terms of local realism. To this end, we introduced the notion of typicality of nonlocality, which turns out to give useful insight into the relation of these sets for a varying number of parties and input settings.

This work is presented in the following way. In the next section we provide an introduction to the numerical method and define nonlocality strength. We also present and discuss an extensive set of numerical results. In Sec. III we explain why the probability of violation depends on the number of measurement settings. In Sec. IV we introduce the concept of typicality of nonlocality, after which we summarize our conclusions.

II. NONLOCALITY STRENGTH

A. Method

In our numerical analysis we consider the most general Bell experiment with N spatially separated observers performing measurements on a given state ρ of N qubits. Each observer can choose between m_i arbitrary dichotomic observables $\{O_1^i, O_2^i, \dots, O_{m_i}^i\}$ ($i = 1, \dots, N$) defined by orthogonal projections $O_j^i = |v_j^+\rangle_i \langle v_j^+| - |v_j^-\rangle_i \langle v_j^-|$ parametrized by the general unitary transformation belonging to $U(3)$ group $|v_j^r\rangle_i = U_j^i |r^i\rangle_i$. For simplicity, we will refer to this scenario as $m_1 \times \dots \times m_N$.

Resistance to noise is understood as the amount of white noise admixture required to completely suppress the nonclassical character of the original correlations of a given state ρ . The state is now described by the following density operator:

$$\rho(v) = v\rho + (1-v)\rho_{\text{white noise}}. \quad (3)$$

The parameter v is called the visibility of the state. For the states that reveal nonclassicality for a particular choice of observables, there always exists a critical visibility v_{crit} , such that for $v \leq v_{\text{crit}}$ a local realistic model can be constructed. The critical visibility provides us with information about noise resistance of quantum correlations. The critical amount of noise for the correlations of a given state becoming local will be called the strength of nonlocality $\mathcal{S} \equiv 1 - v_{\text{crit}}$. This is equivalent to ‘‘white noise robustness,’’ the measure often used in entanglement theory [8].

When we say that an experiment is *nonlocal*, we understand that it has a local realistic model, which is equivalent to the existence of a joint probability distribution $p(r_1^1, \dots, r_{m_1}^1, \dots, r_1^N, \dots, r_{m_N}^N)$, where $r_{j_i}^i \in \{0, 1\}$ denotes the result of the measurement of the i th observer’s $O_{j_i}^i$ observable. If the model exists, quantum probabilities can be expressed by the marginal sums:

$$\begin{aligned} P(r^1, \dots, r^N | O_{k_1}^1, \dots, O_{k_N}^N) \\ &= \text{Tr}[\rho(v) |v_{k_1}^{r_1}\rangle \langle v_{k_1}^{r_1}| \otimes \dots \otimes |v_{k_N}^{r_N}\rangle \langle v_{k_N}^{r_N}|] \\ &= v \text{Tr}(\rho |v_{k_1}^{r_1}\rangle \langle v_{k_1}^{r_1}| \otimes \dots \otimes |v_{k_N}^{r_N}\rangle \langle v_{k_N}^{r_N}|) + \frac{1-v}{2^N} \\ &= \sum_{r_{j_1}^1, \dots, r_{j_N}^N=0}^1 p(r_1^1, \dots, r_{m_1}^1, \dots, r_1^N, \dots, r_{m_N}^N), \quad (4) \end{aligned}$$

where $P(r^1, \dots, r^N | O_{k_1}^1, \dots, O_{k_N}^N)$ denotes the probability of obtaining the result r^i by the i th observer while measuring observables $O_{k_i}^i$ ($i = 1, \dots, N$) on the state (3).

Determining the nonlocality strength, for a given state and set of observables, is a linear programming problem—we maximize $\mathcal{S} = 1 - v$ subject to Eq. (4). Obvious constraints such as normalization of probability and bounding the strength range ($0 \leq \mathcal{S} \leq 1$) are also assumed. An in-depth formulation of this problem and an explanation of the method harnessed to solve it can be found in [9–11]. At this point, we would like to emphasize once again that our method, although numerical, does not need any knowledge at all of the forms of Bell inequalities. However, the results obtained by this method are equivalent to the analysis of the full set of tight Bell inequalities formulated for a given experimental situation.

The nonlocality strength is determined for a particular set of observables used and we report its distribution obtained with a large statistics of random measurements applied to a given state. The measurement operators are sampled according to Haar measure as described in [3, 12].

In comparison with Ref. [3], here we are interested not only in the summary probability that $\mathcal{S} > 0$ for a random observable, but in a detailed probability distribution of achieving a specific value of the nonlocality strength $g(\mathcal{S})$. We should also mention the approach used in [10], where the main goal was to optimize v_{crit} over all possible measurement settings to provide the minimal critical visibility for a given state $v_{\text{crit}}^{\text{min}}$ here relating to the maximal nonlocality strength $\mathcal{S}^{\text{max}} = 1 - v_{\text{crit}}^{\text{min}}$.

The probability of violation \mathcal{P}_V does not provide much information about the strength of nonlocality, on the one hand. On the other hand, resistance against noise, although relevant, is not a proper nonlocality quantifier. A quantity that conveys these two will likely be useful. Therefore, we define the average nonlocality strength:

$$\bar{\mathcal{S}} = \int_0^{\mathcal{S}^{\text{max}}} \mathcal{S} g(\mathcal{S}) d\mathcal{S}. \quad (5)$$

Our results are normalized such that the areas of the regions bounded by the plots directly provide the probabilities of violation, $\int_0^{\mathcal{S}^{\text{max}}} g(\mathcal{S}) d\mathcal{S} = \mathcal{P}_V$.

Alternatively, the above definition can be written as

$$\bar{\mathcal{S}} = \mathcal{P}_V \mathcal{S}^{\text{max}} - \int_0^{\mathcal{S}^{\text{max}}} \mathcal{P}_V(\mathcal{S}) d\mathcal{S}, \quad (6)$$

where $\mathcal{P}_V(\mathcal{S}) = \int_0^{\mathcal{S}} g(\mathcal{S}') d\mathcal{S}'$ is the probability, for a given state ρ , to produce a violation with strength up to \mathcal{S} . Note that $\mathcal{P}_V(\mathcal{S}^{\text{max}}) = \mathcal{P}_V$. This expression makes it clear that we are describing a nonlocality figure of merit in terms of differential slices of the probability of violation. As it is, a more detailed description in the form of closed analytical results are hard to obtain. However, in the case of two maximally entangled qubits some exact relations can be derived.

B. Analytical considerations

Let us first consider the 2×2 scenario. It can be shown that, in this case, $\mathcal{P}_V^{2 \times 2} = 2(\pi - 3) \approx 0.2832$ [1]. In addition, we have $\mathcal{S}^{\text{max}} \leq 1 - 1/\sqrt{2} \approx 0.2929$, since the critical visibility of a Bell state is $1/\sqrt{2}$. Therefore, by replacing \mathcal{S}^{max} in (6) with $1 - 1/\sqrt{2}$ we obtain an upper bound for $\bar{\mathcal{S}}^{2 \times 2}$:

$$\begin{aligned} \bar{\mathcal{S}}^{2 \times 2} &\leq (\pi - 3)(2 - \sqrt{2}) - \int_0^{1-1/\sqrt{2}} \mathcal{P}_V^{2 \times 2}(\mathcal{S}) d\mathcal{S} \\ &\leq (\pi - 3)(2 - \sqrt{2}) \approx 0.0829. \quad (7) \end{aligned}$$

Still referring to two maximally entangled qubits, in the opposite limit of infinitely many settings, $m_1 = m_2 \rightarrow \infty$, v_{crit} is related to $K_G(3)$, the Grothendieck constant of order three, as follows [13]: $K_G(3) = 1/v_{\text{crit}} = 1/(1 - \mathcal{S}^{\text{max}})$. From the known best upper [14] and lower [15] bounds to $K_G(3)$, \mathcal{S}^{max} is bounded as $0.3036 \leq \mathcal{S}^{\text{max}} \leq 0.3171$. With infinitely many settings, one can always find such settings for $\mathcal{S} < \mathcal{S}^{\text{max}}$ that local realism is violated. In addition, Lipinska *et al.* [6] have

shown that in this limit $\mathcal{P}_V \rightarrow 1$, so that we can write

$$\bar{S}^\infty \leq 0.3171 - \int_0^{0.3171} \mathcal{P}_V^\infty(S) dS. \quad (8)$$

For other Bell scenarios, we must resort to numerical calculations (see Supplemental Material [16]). In the next section we present and discuss an extensive set of such computations. Due to the complexity of the data we have to be more descriptive, and the goal is to illustrate the behavior of the quantities introduced here for important states as, for instance, GHZ, W, Dicke, linear (C_4, L_5)—and ring (R_5) clusters, etc., for up to five qubits. All considered states are explicitly defined in the Appendix.

C. Numerical results

Our main numerical results are collected in the form of histograms (Figs. 1–5). The horizontal axis represents the nonlocality strength corresponding to the interval: $[S - 0.01, S)$ and on the vertical axis we have the probability density function (PDF). We recall that all figures are normalized to a random set of settings drawn in the given experiment, so the areas of the regions bounded by the plots are the probabilities of violation.

The following observations can be drawn from the collected results.

1. Two-qubit states

We study two-qubit states of the form $|\text{GHZ}(\alpha)\rangle = \cos \alpha|00\rangle + \sin \alpha|11\rangle$. Note that we can take the above Schmidt form without loss of generality, since the \mathcal{P}_V function is invariant under local unitary transformations.

In Fig. 1 we can observe the distribution characteristic’s dependence on the number of measurement settings m_1 and m_2 , respectively for the first and the second observer. For $m_1 = m_2 \rightarrow \infty$ the plot should look like $\delta(S - S^{\max})$ (compare with [17]). By reducing the number of settings, the distribution blurs and its maximum shifts in the direction of smaller values of S . We observe that, when $m_1 m_2 < 10$, weaker violations are dominant ($\bar{S} \lesssim 0.1$) and for $m_1 m_2 > 10$ this property is reversed.

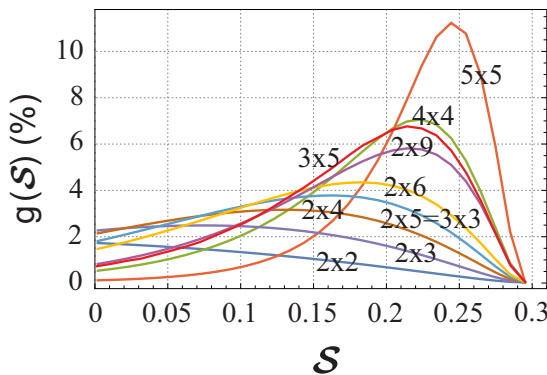


FIG. 1. Nonlocality strength distributions for the two-qubit GHZ state with various quantities of measurement settings for each qubit. Sample size: 10^9 (per state).

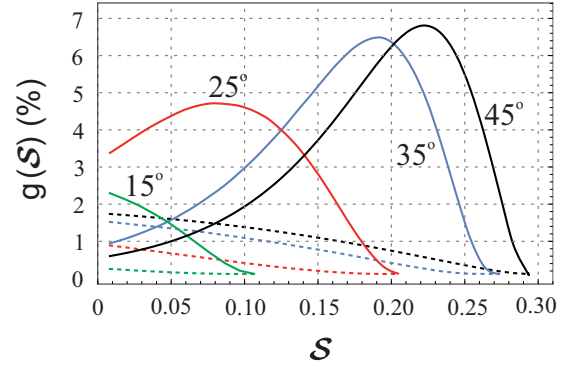


FIG. 2. Nonlocality strength distributions for the two-qubit generalized $\text{GHZ}(\alpha)$ state with 2×2 (dashed) and 4×4 (solid) measurement settings and with selected values of α . Sample size: 10^9 (per state).

We can also notice the coincidence of nonlocality strength distributions for the 2×5 and 3×3 measurement settings (these are the ones with the product closest to each other). It is noted that when ρ in Eq. (3) is the two-qubit maximally entangled state (i.e., $\alpha = 45^\circ$) the single-party expectation values of $\rho(v)$ vanish. In this case our analysis can be restricted to the Bell polytope involving only joint correlation terms. In this reduced space, the polytope is often called the correlation polytope, and the only facets in the $3 \times m$ scenarios for $m \geq 2$ are the variants of the CHSH inequality [18]. Hence the similarity of the curves corresponding to 2×5 and 3×3 scenarios has to relate to statistical considerations: Applying more than two settings for at least one party increases the chance of violation of one of the CHSH-Bell inequalities simply due to statistical reasons. We observe a similar behavior for 3×5 and 4×4 cases.

The maximal nonlocality strength for all considered numbers of settings for $\alpha = 45^\circ$ are constant and equal to $1 - 1/\sqrt{2}$. This value of S^{\max} , corresponding to $v_{\text{crit}} = 1/\sqrt{2}$ for the scenarios $m \times m$ with $m \leq 5$, comes from the studies in Refs. [19,20]. However, the averaged nonlocality strengths decrease or increase with the number of settings and they are equal to 0.028 for 2×2 , 0.110 for 3×3 , 0.178 for 4×4 , and 0.218 for 5×5 scenario.

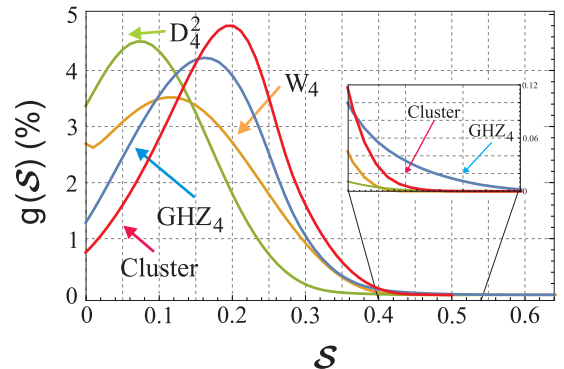


FIG. 3. Nonlocality strength distributions for four-qubit states. Sample size: 10^8 (per state).

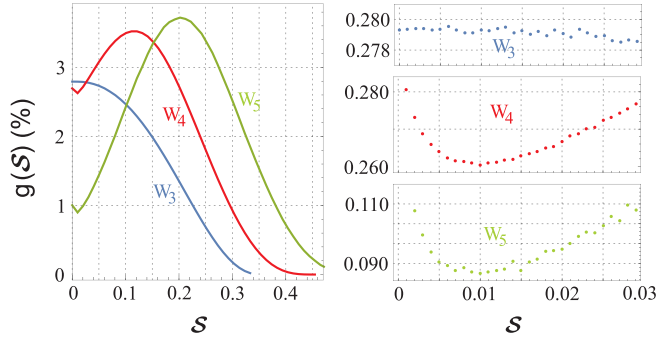


FIG. 4. Unexpected behavior of nonlocality strength distributions close to $S = 0$ for the W states. Sample size: 10^8 (per state).

In Fig. 2 we consider a case $\alpha \neq 45^\circ$. We present two qualitatively different scenarios for 2×2 and 4×4 measurement settings. It confirms a known fact that the maximal nonlocality strength S^{\max} increases with α . Although for a given α , S^{\max} is the same (up to numerical precision) for a scenario with 2×2 and 4×4 measurement settings, the averaged nonlocality strengths for 4×4 scenario are significantly shifted in the direction of higher nonlocality strengths. We also see that the more balanced (α close to $\pi/4$) the state is the higher are the dominant nonlocality strengths.

2. Four- and five-qubit states

For more than two parties, several, inequivalent kinds of entanglement exist. In this subsection we investigate the behavior of some archetypal four- and five-qubit maximally entangled states.

We observe that very strong violations (high nonlocality strength) are more probable for the GHZ state than for other prominent families of four-qubit states (Dicke, W, Cluster). For instance, for nonlocality strength 0.45, the GHZ state violates local realism 7.4 times more likely than the Cluster state. However, the Cluster state surpasses the GHZ state in intermediate values of nonlocality strength (see Fig. 3), where, for example, for $S = 0.35$ the violations are observed 1.7 times more often. This suffices to make the Cluster states attain highest probabilities of violation among all considered states. Also the averaged nonlocality strength

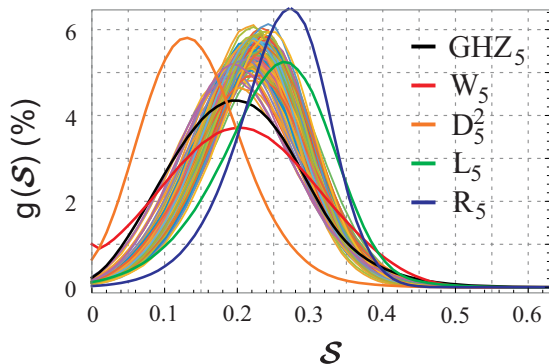


FIG. 5. Nonlocality strength distributions for special and random five-qubit states. Sample size: 10^7 (per state).

for the Cluster state (0.1843) is higher than for the GHZ state (0.1624). Here we considered two settings per party.

When analyzing the histogram for the four-qubit W state we noticed a surprising behavior, namely, a dip for strengths close to 0.02 (see Fig. 4). This was also observed for the five-qubit W state, but not for the three-qubit W state. A possible explanation of this feature could be the fact that there is more than one relevant Bell inequality for the considered cases with different functions representing the nonlocality strength. The total nonlocality strength is a combination of the strengths for those particular inequalities, which may result in several extremes. Of course, this reasoning is valid for any state. What is different about W states is that, as we will see in the next section, more than one family of tight Bell inequalities give sizable contributions to the strength, thus enhancing the effect. On the contrary, e.g., the strength of GHZ states come almost entirely from the CHSH family.

The atypical character of several highly entangled states is illustrated in Fig. 5, where we compare special five-qubit states (GHZ, Dicke, W, and linear- and ring cluster states [21]) with 100 random pure states. The fragility of the Dicke state $|D_5^2\rangle$ in comparison to the other highly entangled states, and even as compared to any of the 100 random states, stands out. So, quantum information protocols that rely on this kind of state, namely, Dicke states with a similar number of 0's and 1's (see also $|D_4^2\rangle$ in Fig. 3), are likely to be very hard to implement in practice. The opposite situation occurs for the ring state $|R_5\rangle$, which presents high nonlocality strength, making it a promising candidate to practical implementation of quantum information protocols. This is a clear illustration of the usefulness of the figure of merit we introduced here, for the probabilities of violation of $|D_5^2\rangle$ and $|R_5\rangle$ are 99.254% and 99.957%, respectively [3], thus giving no clue on the large difference in the strength of these states. In general, the highly entangled states are distinguishable from the random ones either because they have maxima at very different values ($|R_5\rangle, |L_5\rangle, |D_5^2\rangle$) or because they present larger variances ($|GHZ\rangle, |W\rangle$).

III. STATISTICAL RELEVANCE OF FACET INEQUALITIES

One can observe that the probability of violation rapidly increases with the number of measurement settings. We can explain this phenomenon thanks to the fact that our method allows us to identify an explicit form of a Bell inequality, which was violated for given measurement settings.

The first explanation of that fact is statistical. By increasing the number of settings, we increase the probability that some of them violate the Bell inequality involving only two settings (CHSH). For instance, for the experiment with the two qubit GHZ state and five measurement settings per party one can identify the following families of Bell inequalities:

$$\langle a_1 b_1 + a_1 b_2 + a_2 b_1 - a_2 b_2 \rangle \leq 2, \quad (9)$$

$$\langle a_1 b_1 - a_3 b_1 + a_4 b_1 + a_5 b_1 - a_3 b_2 - a_4 b_2 - a_1 b_4 + a_3 b_4 - a_4 b_4 + a_5 b_4 2a_1 b_5 - a_3 b_5 + a_4 b_5 \rangle \leq 6, \quad (10)$$

$$\langle a_1 b_1 + a_2 b_1 - a_4 b_1 - a_5 b_1 - a_1 b_3 + a_2 b_3 - a_4 b_3 + a_5 b_3 - a_1 b_4 + a_2 b_4 - 2a_3 b_4 + a_4 b_4 - a_5 b_4 \rangle$$

$$\begin{aligned}
& -a_1b_5 + a_2b_5 + 2a_3b_5 + a_4b_5 - a_5b_5 \leq 8, \quad (11) \\
& \langle -a_1b_1 - a_2b_1 - a_3b_1 + 2a_4b_1 + a_5b_1 + a_1b_2 \\
& + a_4b_2 - a_5b_2 + a_1b_3 - a_3b_3 + a_4b_3 - a_5b_3 \\
& - a_3b_4 + a_4b_4 + 2a_5b_4 + 2a_3b_5 + a_4b_5 + a_5b_5 \\
& + a_2b_4 + a_3b_2 + a_1b_4 \rangle \leq 10. \quad (12)
\end{aligned}$$

Here $\langle a_i b_j \rangle$ denotes an expectation value of the correlation measurement in which the first and the second observers measure observables a_i and b_j , respectively. Each family contains many equivalent inequalities. For example, the first family (9) is obtained by replacing settings $a_i \rightarrow \pm a_k$ and $b_j \rightarrow \pm b_l$, where $k, l \in \{1, 2, 3, 4, 5\}$.

We note that all the above Bell inequalities are tight, that is, they define facets of the Bell local polytope (and they are facets of the correlation polytope too). The inequality (10) is a genuine (4×5) -setting Bell inequality, whereas (11) and (12) are genuine (5×5) -setting Bell inequalities.

The highest violation strength is observed for inequalities belonging to family (9) in 99.1% of random sets of settings, (10) in 0.85%, (11) in 0.04%, and (12) in 0.01%. This means that in almost all cases we effectively use only two out of five settings.

A distinct effect is observed in the case of the three-qubit W state. In this case 14% of observed violations really involve three measurement settings. One of the examples of a genuine $3 \times 3 \times 3$ inequality is

$$\begin{aligned}
& \langle a_1 + 5a_2 - 5a_3 + b_1 - a_1b_1 - a_2b_1 + 3a_3b_1 + 3b_2 + a_1b_2 \\
& - 2a_3b_2 + b_3 + a_1b_3 + c_1 - 2a_1c_1 - 2a_2c_1 + a_3c_1 + 2b_1c_1 \\
& + 4a_1b_1c_1 - a_2b_1c_1 + a_3b_1c_1 - 2b_2c_1 + 2a_1b_2c_1 + 3a_2b_2c_1 \\
& - 3a_3b_2c_1 - 5b_3c_1 + 4a_2b_3c_1 - 3a_3b_3c_1 + a_2c_2 + a_3c_2 \\
& + a_1b_1c_2 - 3a_2b_1c_2 - 2a_3b_1c_2 - 3b_2c_2 - 3a_3b_2c_2 + 3b_3c_2 \\
& + a_1b_3c_2 - 4a_2b_3c_2 + 2c_3 + a_1c_3 - 2a_2c_3 + a_3c_3 - 3b_1c_3 \\
& - 2a_1b_1c_3 + a_2b_1c_3 - 4a_3b_1c_3 + 2b_2c_3 - 3a_1b_2c_3 \\
& + 3a_2b_2c_3 + 2a_3b_2c_3 - 3b_3c_3 - 3a_3b_3c_3 \rangle \leq 23. \quad (13)
\end{aligned}$$

IV. TYPICALITY OF NONLOCALITY

It is known that the set of multipartite entangled states is large [22]. Obviously almost all random pure states are entangled and, even more, most of them are sufficiently entangled to be useful as computational resources [23]. Now one can ask a similar question concerning a more demanding property—nonlocality. What is the typical probability of violation T_V for a randomly sampled pure state? In this problem we specify only the number of qubits N and the Bell scenario. It is known that any pure entangled state violates Bell inequalities [24,25]. However, measurement settings that lead to the violation are carefully selected. We consider another scenario, in which for any random state we choose only one random set of settings. For a given pure state $|\psi(\theta, \phi)\rangle = \cos \theta |00\rangle + e^{i\phi} \sin \theta |11\rangle$ we verify the violation only for a single randomly chosen set of settings (in the space Ω). The states are uniformly sampled

TABLE I. Typical probability of violation T_V and typical nonlocality strength T_S for pure random qubit states and random measurements (one random measurement per random state).

N	Settings	Statistics	T_V (%)	T_S
2	2×2	10^9	5.32	0.004
	3×3	10^9	21.99	0.019
	4×4	10^8	38.43	0.038
	5×5	10^7	50.04	0.054
	6×6	10^7	57.98	0.068
	7×7	10^6	63.63	0.079
	8×8	10^5	67.83	0.087
	9×9	10^4	71.23	0.093
	10×10	10^4	74.34	0.097
	11×11	10^3	76.80	0.101
	3	$2 \times 2 \times 2$	10^7	42.96
4	$2 \times 2 \times 2 \times 2$	10^8	93.28	0.123
5	$2 \times 2 \times 2 \times 2 \times 2$	10^7	99.88	0.222
6	$2 \times 2 \times 2 \times 2 \times 2 \times 2$	10^6	>99.99	0.306
7	$2 \times 2 \times 2 \times 2 \times 2 \times 2 \times 2$	10^4	>99.99	0.377

on the surface of the Bloch sphere. The typicality is given by $T_V = N_{F=1}/N$, where here N is the total number of samplings and $N_{F=1}$ is the number of times local realism is violated:

$$F[|\psi(\theta, \phi)\rangle, \Omega] = \begin{cases} 1, & \text{if local realism} \\ & \text{is violated,} \\ 0, & \text{otherwise.} \end{cases} \quad (14)$$

We will also compute the averaged strength T_S in this more general situation.

For two observers we analyze experiments up to 11 settings per side. As expected the typicality grows as m_1 and m_2 increase, though at a very slow rate. However, since $\mathcal{P}_V \rightarrow 1$ for any entangled pure two-qubit states as $m_1 = m_2 \rightarrow \infty$ [6], it follows that $T_V \rightarrow 1$ in this limit. The typical strength T_S is quite low for a small number of parties, but grows much faster with increasing N (about two orders of magnitude in the investigated range).

For three and more observers, we employed Bell scenarios involving only two measurement settings. The results are presented in the lower part of Table I. Already for $N = 4$ we observe a quite high typical probability of violation ($T_V > 93\%$). For $N > 4$ it is practically equal to 100%. This means that almost all states violate local realism for any settings. The result seems to be stronger than in the case of “typicality of entanglement,” where measurements are optimized. Also, the typical nonlocality strength T_S increases with the number of parties and settings. The value of T_S for two qubits and infinitely many measurement settings can be bounded from below by 0.1436. This lower bound value comes from an analytical treatment in which one assumes that all facets of the corresponding Bell polytope are defined only by the variants of the CHSH inequalities. The nonlocality strength can be calculated using Horodecki’s formula [26] and averaging over all pure random states.

The use of probabilistic tools is a promising approach to study the typicality of Bell nonlocality [27,28]. For instance, Ref. [27] has found that the probability that a multipartite system with local dimension d violates any N -party, m -setting, o -outcome Bell inequality goes to zero asymptotically in N . However, in the proof of Ref. [27], d has to be larger than $om(2m-1)^2$. That is, applying the analytical results of Ref. [27] to our case of $m=o=2$ would require at least local dimension $d=36+1$. Complementary to [27], our paper gives insight into the geometry of Bell correlations in the case of multiqubit systems fully based on numerically obtained results.

V. CLOSING REMARKS

In this paper we employed linear programming as a useful tool to analyze the nonclassical properties of quantum states. We introduced nonlocality strength as a resistance to white noise admixture and verify its statistical properties. Most of the conclusions were presented in the previous sections. Here we want to stress that the overall message of the obtained results is that nonlocality is a typical phenomenon for multipartite states, i.e., the probability that a random multipartite state violates some Bell inequality for a random set of measurement settings is close to one.

ACKNOWLEDGMENTS

We thank L. Knips and H. Weinfurter for valuable discussions. W.L. acknowledges the support by DFG (Germany) and NCN (Poland) within the joint funding initiative “Beethoven2” (Grant No. 2016/23/G/ST2/04273). J.G. and W.L. acknowledge partial support by the Foundation for Polish Science (IRAP project, ICTQT, Contract No. 2018/MAB/5, cofinanced by EU via Smart Growth Operational Programme). F.P. acknowledges financial support from Coordenação de Aperfeiçoamento de Pessoal de Nível Superior (CAPES), Fundação de Amparo à Ciência e Tecnologia do Estado de Pernambuco (FACEPE), and Conselho Nacional de Desenvolvimento Científico e Tecnológico, through its program CNPq INCT-IQ (Grant No. 465469/2014-0). T.V. was supported by the National Research, Development and Innovation Office NKFIH (Grant No. KH125096).

APPENDIX : STATES UNDER CONSIDERATION

Below we present the set of states for which statistical properties of the nonlocality strength have been analyzed:

$$|\text{GHZ}_2\rangle = (|00\rangle + |11\rangle)/\sqrt{2}, \quad (\text{A1})$$

$$|\text{GHZ}_3\rangle = (|000\rangle + |111\rangle)/\sqrt{2}, \quad (\text{A2})$$

$$|\text{W}_3\rangle = (|001\rangle + |010\rangle + |100\rangle)/\sqrt{3}, \quad (\text{A3})$$

$$|\text{GHZ}_4\rangle = (|0000\rangle + |1111\rangle)/\sqrt{2}, \quad (\text{A4})$$

$$|\text{W}_4\rangle = (|0001\rangle + |0010\rangle + |0100\rangle + |1000\rangle)/2, \quad (\text{A5})$$

$$|D_4^2\rangle = (|0011\rangle + |0101\rangle + |0110\rangle + |1001\rangle + |1010\rangle + |1100\rangle)/\sqrt{6}, \quad (\text{A6})$$

$$|\text{Cluster}\rangle = (|0000\rangle + |1100\rangle + |0011\rangle - |1111\rangle)/2, \quad (\text{A7})$$

$$|\text{GHZ}_5\rangle = (|00000\rangle + |11111\rangle)/\sqrt{2}, \quad (\text{A8})$$

$$|\text{W}_5\rangle = (|00001\rangle + |00010\rangle + |00100\rangle + |01000\rangle + |10000\rangle)/\sqrt{5}, \quad (\text{A9})$$

$$|D_5^2\rangle = (|00011\rangle + |00101\rangle + |00110\rangle + |01001\rangle + |01010\rangle + |01100\rangle + |10001\rangle + |10010\rangle + |10100\rangle + |11000\rangle)/\sqrt{10}, \quad (\text{A10})$$

$$|L_5\rangle = (|00000\rangle + |00010\rangle + |00101\rangle - |00111\rangle + |01000\rangle + |01010\rangle + |01101\rangle - |01111\rangle + |10001\rangle - |10011\rangle + |10100\rangle + |10110\rangle - |11001\rangle + |11011\rangle - |11100\rangle - |11110\rangle)/4, \quad (\text{A11})$$

$$|R_5\rangle = (|00001\rangle + |00010\rangle + |00100\rangle - |00111\rangle + |01000\rangle + |01011\rangle + |01101\rangle - |01110\rangle + |10000\rangle - |10011\rangle + |10101\rangle + |10110\rangle - |11001\rangle + |11010\rangle - |11100\rangle - |11111\rangle)/4. \quad (\text{A12})$$

-
- [1] Y.-C. Liang, N. Harrigan, S. D. Bartlett, and T. Rudolph, *Phys. Rev. Lett.* **104**, 050401 (2010).
- [2] E. A. Fonseca and F. Parisio, *Phys. Rev. A* **92**, 030101(R) (2015).
- [3] A. de Rosier, J. Gruca, F. Parisio, T. Vértesi, and W. Laskowski, *Phys. Rev. A* **96**, 012101 (2017).
- [4] A. Fonseca, A. de Rosier, T. Vértesi, W. Laskowski, and F. Parisio, *Phys. Rev. A* **98**, 042105 (2018).
- [5] A. Barasiński and M. Nowotarski, *Phys. Rev. A* **98**, 022132 (2018).
- [6] V. Lipinska, F. J. Curchod, A. Máttar, and A. Acín, *New J. Phys.* **20**, 063043 (2018).
- [7] A. Canabarro, S. Brito, and R. Chaves, *Phys. Rev. Lett.* **122**, 200401 (2019).
- [8] V. Scarani, *Bell Nonlocality* (Oxford University Press, Oxford, 2019).
- [9] D. Kaszlikowski, P. Gnaniński, M. Żukowski, W. Miklaszewski, and A. Zeilinger, *Phys. Rev. Lett.* **85**, 4418 (2000).
- [10] J. Gruca, W. Laskowski, M. Żukowski, N. Kiesel, W. Wieczorek, C. Schmid, and H. Weinfurter, *Phys. Rev. A* **82**, 012118 (2010).
- [11] J. Gondzio, J. A. Gruca, J. A. J. Hall, W. Laskowski, and M. Żukowski, *J. Comput. Appl. Math.* **263**, 392 (2014).
- [12] K. Życzkowski and M. Kuś, *J. Phys. A* **27**, 4235 (1994).

- [13] A. Acin, N. Gisin, and B. Toner, *Phys. Rev. A* **73**, 062105 (2006).
- [14] F. Hirsch, M. T. Quintino, T. Vértesi, M. Navascués, and N. Brunner, *Quantum* **1**, 3 (2017).
- [15] P. Diviánszky, E. Bene, and T. Vértesi, *Phys. Rev. A* **96**, 012113 (2017).
- [16] See Supplemental Material at <http://link.aps.org/supplemental/10.1103/PhysRevA.101.012116> for the computer code used to obtain all presented numerical results.
- [17] C. Duarte, S. Brito, B. Amaral, and R. Chaves, *Phys. Rev. A* **98**, 062114 (2018).
- [18] A. Garg, *Phys. Rev. D* **28**, 785 (1983).
- [19] M. Deza and M. Dutour Sikirić, *Optim. Lett.* (2018), doi:[10.1007/s11590-018-1358-3](https://doi.org/10.1007/s11590-018-1358-3).
- [20] S. Kinnewig, Bachelor thesis, Leibniz Universität Hannover, Germany, 2017.
- [21] M. Hein, J. Eisert, and H. J. Briegel, *Phys. Rev. A* **69**, 062311 (2004).
- [22] S. J. Szarek, *Phys. Rev. A* **72**, 032304 (2005).
- [23] D. Gross, S. T. Flammia, and J. Eisert, *Phys. Rev. Lett.* **102**, 190501 (2009).
- [24] S. Popescu and D. Rohrlich, *Phys. Lett. A* **166**, 293 (1992).
- [25] M. Gachechiladze and O. Gühne, *Phys. Lett. A* **381**, 1281 (2017).
- [26] R. Horodecki, P. Horodecki, and M. Horodecki, *Phys. Lett. A* **200**, 340 (1995).
- [27] R. C. Drumond, C. Duarte, and R. I. Oliveira, *J. Math. Phys.* **59**, 052202 (2018).
- [28] C. E. González-Guillén, C. Lancien, C. Palazuelos, and I. Villanueva, *Ann. Henri Poincaré* **18**, 3793 (2017).